COMPDYN 2025
10th ECCOMAS Thematic Conference on
Computational Methods in Structural Dynamics and Earthquake Engineering
M. Papadrakakis, M. Fragiadakis (eds.)
Rhodes Island, Greece, 15-18 June 2025

COMPARATIVE LIFE-CYCLE COST ANALYSIS OF EXISTING STEEL FRAMES RETROFITTED WITH DIFFERENT BUCKLING-RESTRAINED BRACE DESIGNS

Giulia Giuliani[1], **Fernando Gutiérrez-Urzúa**[1,2], **Roberto Gentile**[3] **and Fabio Freddi**[1]

[1] Department of Civil, Environmental and Geomatic Engineering, University College of London
UCL, London, UK
g.giuliani,f.freddi@ucl.ac.uk

[2] AtkinsRéalis, Epsom, UK
fernando.gutierrezurzua@atkinsrealis.com

[3] Institute for Risk and Disaster Reduction, University College London, London, United Kingdom
r.gentile@ucl.ac.uk

Abstract

Most existing buildings were constructed before the implementation of modern seismic design codes and their design often lacks considerations for lateral resistance. These structures are often unable to withstand seismic events, posing a significant risk to public safety and leading to considerable direct (e.g., casualties, repair costs) and indirect (e.g., downtime) losses as a consequence of 'rare' (i.e., high-intensity) seismic events. In this context, there is a significant need for effective retrofitting methods and decision-making strategies to enhance the seismic performance of these structures. However, designing such upgrades requires careful consideration of the trade-off between their cost and the associated economic benefits. This study provides a methodology to design optimal retrofit solutions for existing (i.e., non-seismically designed) steel Moment-Resisting Frames (MRFs) using Buckling Restrained Braces (BRBs). This is achieved by examining various BRB designs through life-cycle cost analysis, which includes the costs associated with retrofitting and potential structural and non-structural repairs following a seismic event. The optimal retrofit allows balancing the reduction of seismic risk with the long-term economic benefits, and it is selected considering various key metrics, including Life-Cycle Cost (LCC), Benefit-to-Cost Ratio (BCR) and Return on Investment (ROI). The results demonstrate that using BRBs as a retrofit strategy effectively minimises structural and non-structural damage, leading to significant reductions in LCC. Furthermore, the most cost-effective BRB design is identified among the proposed solutions.

Keywords: Seismic Retrofit, Buckling Restrained Braces, Life-Cycle Cost Analysis, Structural Resilience.

1 INTRODUCTION

Most existing buildings worldwide have been designed before the introduction of modern seismic design codes and need retrofitting. For example, in Europe, more than 80% of the buildings preceded the implementation of contemporary seismic design codes and may show a poor seismic performance [1]. These structures often lack capacity design, exhibit low ductility, and possess inadequate energy dissipation capabilities, making them highly vulnerable to earthquakes and posing significant risks to their occupants. Moreover, such inadequate designs often lead to high direct (*e.g.,* injuries, casualties, repair cost) and indirect (*e.g.,* downtime, stock exchange drop) losses after high-intensity seismic events.

In this context, there is a pressing demand for efficient retrofitting methods and robust decision-making strategies to improve the seismic performance of these structures. Over the last few decades, several innovative retrofitting methods have been developed, including *i)* seismic isolation [2–4] or *ii)* passive energy dissipation (*e.g.,* bracing dissipative systems [5–7], added damping and stiffness devices [8,9], triangular-plate added damping and stiffness devices [10,11]). These technologies allow the opportunity to preserve both structural and non-structural components from damage, hence contributing to the enhancement of seismic resilience [12]. Among others, Buckling Restrained Braces (BRBs) represent an effective solution for the seismic retrofitting of existing structures due to their large energy dissipation capacity and stable hysteretic behaviour. These devices are often included in series with elastic braces and placed within the frames of the existing structures. BRBs are composed of a sleeve that prevents an unbonded core from buckling. As buckling is prevented, the BRB's core can yield axially, both in tension and compression, thereby inducing an almost symmetric hysteretic response [13,14]. Their applicability as a retrofit strategy has been proven for both steel and reinforced concrete structures through extensive experimental [15,16] and numerical studies [17–22].

Although the effectiveness of such retrofit strategies has been well-documented, their widespread implementation is often constrained by economic resources. Hence, a thorough evaluation of retrofitting costs, the associated economic benefits, and a strategic optimisation of the resources is required to implement these strategies. In this context, a risk-based Life-Cycle Cost (LCC) analysis constitutes a robust framework for the economic evaluation of seismic retrofit strategies. LCC encompasses all costs incurred over a structure's lifetime, including initial construction, maintenance, repair, and eventual demolition. Of particular importance is the repair cost following extreme seismic events, which can significantly impact the overall economic feasibility of the retrofit. In previous studies, LCC has been used to identify the most cost-effective structural control systems [23]. In other studies, LCC has been used as a parameter in a multi-objective optimisation procedure for the identification of the optimal seismic design [24]. The LCC has been employed as a methodology to evaluate the best retrofit techniques not only for buildings [25], but also for bridges [26]. Parallel with LCC, the cost-benefit analysis is another key tool in evaluating the financial viability of seismic retrofitting strategies [27,28]. By explicitly quantifying the relationship between mitigation effectiveness and associated costs, these assessments support investments in seismic safety that are both technically sound and economically justifiable.

This study aims to evaluate and compare the LCC of different BRB retrofitting designs for existing steel Moment-Resisting Frames (MRFs). While the upfront investment in retrofitting can be substantial, LCC analysis provides a holistic view of the financial impact over the entire service life of a structure. Furthermore, an extensive examination of additional key metrics, including the Benefit-to-Cost Ratio (BCR) and the Return on Investment (ROI), was conducted. This multifaceted approach was undertaken to ensure a comprehensive evaluation of each retrofit measure, thereby facilitating the identification of the optimal design. The results of this

study provide a framework that allows for balancing the cost, *i.e.*, initial retrofitting investment, with the lifetime benefits, *i.e.*, reduction in risk, vulnerability, and expected losses of a structure.

2 METHODOLOGY

The most cost-effective retrofit design of the BRBs was identified through the following methodology. First, a non-seismically designed steel MRF was selected for case study purposes and modelled in the finite element software OpenSees [29]. The seismic performance of the existing structure was evaluated, and seven different retrofit designs, consistent with the same target spectrum, were developed. The design was carried out considering the steel MRF and the BRBs to work in parallel as a dual system. The MRF structure was reduced to an equivalent single degree of freedom [30] and the properties of the system were identified through an iterative procedure [20,31]. Successively, the stiffness and ductility of the system were calibrated, aiming to have a concurrent failure of all BRBs at a target top-story drift. At the same time, the strength of the BRBs was calibrated to produce the simultaneous yielding of the devices. The BRBs are made by a series arrangement of a BRB device and a steel brace designed to remain elastic [32]. This solution enables the independent calibration of the strength and stiffness of the BRBs. Additional details can be found in Gutiérrez-Urzúa and Freddi [20].

The seismic performance of the structure was assessed through non-linear time history analyses based on an Incremental Dynamic Analysis (IDA) [33]. In particular, the structures were subjected to a suite of representative ground motion records scaled to multiple intensity levels. Successively, fragility functions were defined by monitoring various Engineering Demand Parameters (EDPs) and considering different Damage States (DSs). These tools provide the probability of entering a specified DS (or exceeding a specified Limit State), conditional to the strong-motion shaking severity, quantified by means of an appropriately selected Intensity Measure (*IM*). Fragility functions were derived according to standard methodologies [34] and described by a lognormal cumulative distribution function. Following the evaluation of seismic performance, the vulnerability of the structure can be assessed. This paper derives vulnerability functions, which establish the relationship between the losses and an *IM*, by considering the repair costs associated with each DS. Specifically, the vulnerability function is calculated by multiplying the repair cost of each DS by the probability of the structure being in that DS for a given *IM*. The total repair cost of the structure at a given *IM*, *i.e.*, the mean vulnerability function, is then determined by aggregating the vulnerability curves of all DSs at each *IM*, as follows:

$$V_i(im) = P(DS_i|im) \cdot cost(DS_i) \qquad V(im) = \sum_i V_i\,(im) \tag{2}$$

where $P(DS_i|im)$ is the probability of being in DS_i conditional to the *IM* value *im*, *i.e.*, the fragility function, $cost(DS_i)$ is the repair cost of DS_i, typically expressed as a percentage of the replacement cost of the entire structure, $V_i(im)$ is the vulnerability function associated with DS_i, while $V(im)$ is the aggregated vulnerability function considering all DSs.

Convoluting the vulnerability function and the seismic hazard curve provides the Expected Annual Loss (EAL). This is defined as the average monetary loss expected in a year due to seismic risk, and can be calculated as follows:

$$\mathrm{EAL} = \int V(im) \cdot \lambda(im)\, dIM \tag{3}$$

where $\lambda(im)$ represents the annual frequency of exceedance of earthquakes with intensity *im*.

The LCC analysis in this study is limited to the costs associated with potential seismic damage. Costs related to building maintenance and initial construction are excluded, as they are common to all retrofitted structures and therefore do not contribute to identifying the most cost-

effective retrofit design. Consequently, the LCC considering seismic losses and initial retrofitting costs, can be calculated as follows:

$$\mathrm{LCC} = \frac{(1+r)^{T_N}-1}{r} \cdot \mathrm{EAL} + C_R \tag{4}$$

where r is the annual discount rate, taken equal to 5%, T_N is the expected lifetime of the building, and C_R is the initial cost of the retrofitting design.

An additional key metric for evaluating the economic efficiency of the retrofitting design is the Benefit-to-Cost Ratio (BCR). This is the ratio of the benefits gained (*i.e.*, the reduced LCC) to the costs incurred (*i.e.*, initial retrofitting investment) as follows:

$$\mathrm{BCR} = \frac{Benefit}{Cost} = \frac{\mathrm{LCC}_{bare} - \mathrm{LCC}_{retrofit}}{C_R} \tag{5}$$

A BCR greater than 1 indicates that the financial benefits of retrofitting outweigh the costs, making it a cost-effective design. By comparing different retrofitting strategies using BCR, decision-makers can identify the most efficient investment, ensuring maximum risk reduction while optimising financial resources. Finally, the ROI is considered as it indicates the time required to recover the initial retrofitting cost and helps investors assess profitability. ROI is thus calculated as the time t, such that the cumulative EAL up to t equals the retrofit cost. A lower ROI suggests that the retrofitting design offers significant long-term savings relative to its upfront cost, making it a financially viable choice.

3 CASE STUDY STRUCTURE AND FINITE ELEMENT MODELLING

The case study structure is based on the pre-Northridge Boston 3-story structure developed as part of the SAC-FEMA Steel Project [35]. This structure is representative of low-code steel MRF, as it was designed considering gravity, wind, and low seismic demands. The design assumes stiff soil conditions, office occupancy, a regular plan layout, and no significant irregularities along the height. Additionally, only the perimeter frames were designed to resist lateral loads, with internal frames acting solely as gravity frames, which reflects standard practices in the early 1990s in the United States. For this study, only one of the North-South external MRFs is analysed, as the building's symmetry eliminates the need to assess multiple frames. The geometry of the case study and the steel profiles used can be found in Figure 1.

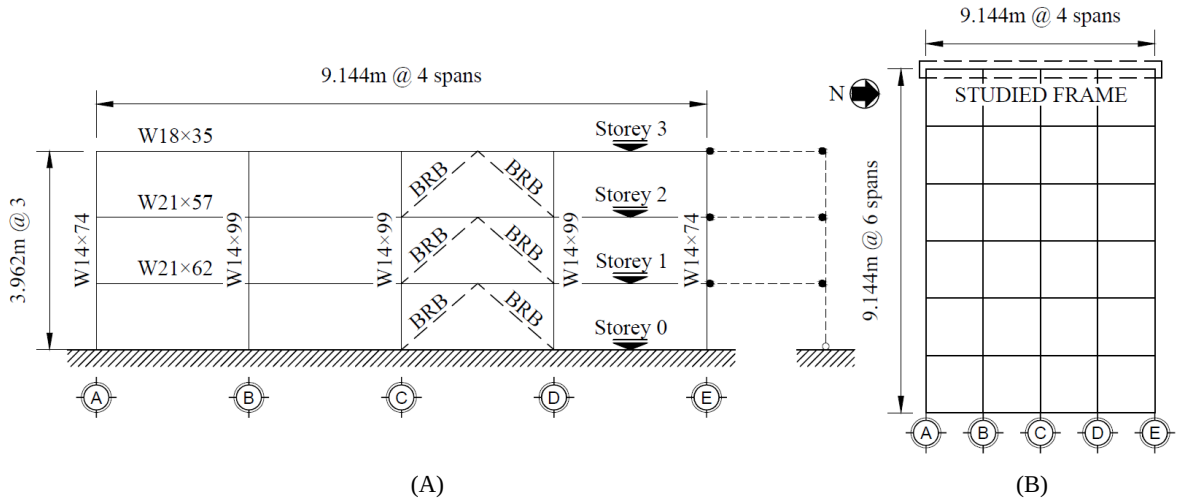

Figure 1: Case study structure: (A) elevation view, (B) plan view. [Adapted from Gutiérrez-Urzúa and Freddi [20]].

The retrofitting focuses on enhancing the seismic performance of the structure to meet a specified higher seismic demand. For this purpose, the seismic hazard characteristics of Los Angeles (see Figure 2) are considered. The seismic performance assessment of the existing structure and the BRBs' retrofit design has been thoroughly investigated by Gutiérrez-Urzúa and Freddi [20]. A chevron (inverted 'V') BRBs configuration was chosen by the authors, as illustrated in Figure 1(a). Seven BRBs' designs are developed based on different target top-story drifts and DSs, *i.e.*, Immediate Occupancy (IO), Life Safety (LS), and Collapse Prevention (CP), defined according to ASCE 41-17 [36]. The lower bound (*i.e.*, low target drift – Case study R1) prioritises protecting the MRF from damage, ensuring all MRF elements remain within the IO DS. This approach enhances structural resilience and facilitates easy repairs by simply replacing the BRBs. The upper bound (*i.e.*, large target drift – Case study R7) represents a design objective where the MRF plays a more significant role in the dual system's capacity, allowing damage to the existing elements and exploiting their energy dissipation capacity. In this scenario, MRF elements exceed the IO level but are expected to remain below the CP threshold. To explore intermediate performance scenarios, five additional target top-story drift values are considered. For the sake of completeness, the BRBs' dimensions resulting from the design and the corresponding fundamental vibration periods are reported in Table 1.

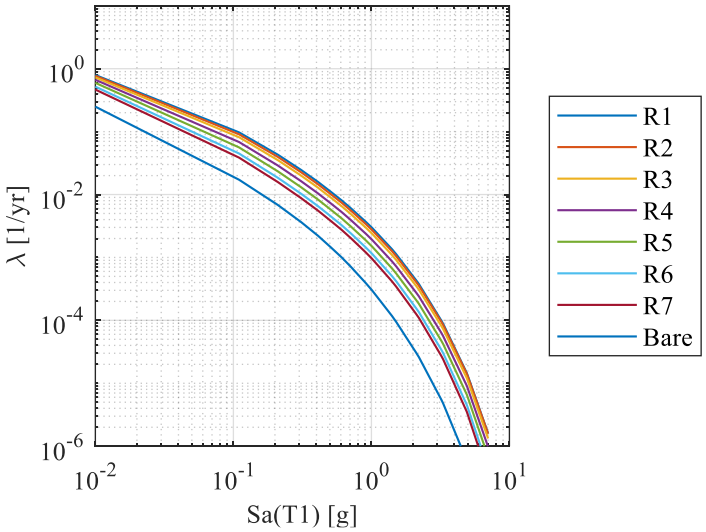

Figure 2: Hazard curves for Los Angeles, site Class D, by considering the fundamental periods of the bare and retrofitted schemes. The curves corresponding to the periods of interest are linearly interpolated from the λ for adjacent periods.

	BRBs Area [cm^2]			BRBs Length [m]			T_1
Storey	1st	2nd	3rd	1st	2nd	3rd	[s]
R1	109.0	93.4	58.1	0.73	0.92	0.85	0.48
R2	82.7	70.9	44.1	1.09	1.38	1.28	0.53
R3	60.2	51.5	32.0	1.45	1.84	1.70	0.60
R4	43.4	37.2	23.1	1.82	2.30	2.13	0.70
R5	31.4	26.9	16.7	2.18	2.76	2.55	0.82
R6	22.8	19.5	12.1	2.54	3.21	2.98	0.96
R7	15.9	13.6	8.5	2.91	3.67	3.40	1.11
Bare	/	/	/	/	/	/	1.88

Table 1: BRBs' characteristics and first natural vibration periods of the structures.

A two-dimensional model of the perimeter MRF has been developed by Gutiérrez-Urzúa and Freddi [20] in the FE software OpenSees. The column bases are modelled as fixed, while the column elements are modelled using a distributed plasticity approach to capture the interaction of axial and bending stresses. Beams are modelled with a lumped plasticity approach, consisting of non-linear rotational springs combined with elastic beam elements. The plastic hinges in the beams are calibrated based on the model proposed by Lignos and Krawinkler [37] and modified as suggested by Zareian and Medina [38]. Panel zones are modelled according to the 'Scissors model' [39] using two parallel rotational springs. The BRB devices are modelled using *corotTrussSection* elements, characterised by the *SteelBRB* material [14]. Moreover, a leaning column is linked to the structure by rigid truss elements, as shown in Figure 1(a), to account for the presence of the gravity frames and account for the related P-Δ effects.

The seismic performance was assessed through non-linear time-history analyses using a set of 30 spectra-compatible accelerograms in an IDA fashion, after which fragility curves were derived. Rotations of beams, columns, and panel zones were regarded as local EDPs and the associated limit states were defined according to ASCE 41-17 [36]. Moreover, the spectral acceleration corresponding to the first natural vibration period, $S_a(T_1)$, was considered as *IM*. Finally, the non-structural component assessment was performed considering both drift-sensitive and acceleration-sensitive components and monitoring maximum-over-time of, respectively, the interstorey drift and the acceleration in all storeys. To establish the limit state for non-structural DSs, the HAZUS 4.2 Technical Manual [40] has been used as a reference. In particular, Slight (S), Moderate (M), Extensive (E) and Complete (C) DSs were considered.

Table 2, Table 3 and Table 4 reports the fragility curve parameters, *i.e.*, mean IM_{50} and dispersion β, for structural, non-structural drift-sensitive and acceleration-sensitive components.

Table 2 reports the fragility curve parameters for structural components. It is noteworthy that the DSs for LS and CP are reported in a single column. This is due to the fact that for the considered case study structure, these DSs are related to the demand in the panel zones for which the ASCE 41-17 [36] provides identical capacity values for LS and CP. Table 2 shows that the R1 design, characterised by the 'biggest' BRBs, exhibits the highest IM_{50} values. Additionally, the IM_{50} value for the BRBs aligns closely with those of the IO DS, as intended from the design. Conversely, the R7 design shows substantially lower IM_{50} values. However, it is noteworthy that IM_{50} values for CP of R7 are aligned with the IM_{50} value for IO of R1. Additionally, the IM_{50} value of the BRBs of R7 corresponds to that of CP, as expected from the design. The β values are relatively consistent among different DSs; however, higher values are observed in the case of severe DSs.

	IM_{50} [g]			β		
DS	IO	LS-CP	BRB	IO	LS-CP	BRB
R1	1.58	3.31	1.39	0.28	0.59	0.28
R2	1.25	3.04	1.45	0.29	0.36	0.33
R3	0.87	2.41	1.28	0.31	0.40	0.30
R4	0.69	2.05	1.25	0.34	0.41	0.36
R5	0.61	1.82	1.24	0.38	0.38	0.38
R6	0.48	1.54	1.17	0.32	0.49	0.39
R7	0.35	1.21	1.03	0.28	0.42	0.37
Bare	0.10	0.43	/	0.12	0.34	/

Table 2: Structural components' fragility parameters for the Damage States (DSs): Immediate Occupancy (IO), Life Safety (LS) and Collapse Prevention (CP).

Table 3 reports the IM_{50} and β values for non-structural drift-sensitive components, showing that performance improvements correlate directly with the size, *i.e.*, the stiffness and strength, of the BRBs. In contrast, for non-structural acceleration-sensitive components, as detailed in Table 4, retrofit designs generally exhibit comparable values except for the Slight DS. These similar results stem from the dual effects provided by the BRBs which, from one side provide an increased energy dissipation capacity, reducing the accelerations, and on the other side, increase the stiffness of the structure, thereby reducing the period and increasing the demand. Additional details on the numerical model and analyses can be found in Gutiérrez-Urzúa and Freddi [20].

	IM_{50} [g]				β			
DS	S	M	E	C	S	M	E	C
R1	0.62	1.31	3.31	3.31	0.14	0.28	0.59	0.59
R2	0.44	1.03	2.74	3.11	0.19	0.31	0.37	0.35
R3	0.34	0.70	1.98	2.89	0.17	0.36	0.36	0.45
R4	0.26	0.54	1.56	2.60	0.23	0.35	0.41	0.44
R5	0.19	0.43	1.29	2.25	0.13	0.34	0.40	0.39
R6	0.12	0.34	1.02	1.83	0.23	0.23	0.34	0.49
R7	0.09	0.23	0.78	1.40	0.30	0.25	0.33	0.43
Bare	0.03	0.06	0.27	0.47	0.12	0.13	0.34	0.36

Table 3: Non-structural drift-sensitive components' fragility parameters for the Damage States (DSs): Slight (S), Moderate (M), Extensive (E), and Complete (C).

	IM_{50} [g]				β			
DS	S	M	E	C	S	M	E	C
R1	0.22	0.42	1.05	2.54	0.09	0.05	0.21	0.44
R2	0.20	0.39	1.10	2.40	0.11	0.17	0.45	0.40
R3	0.16	0.42	1.14	2.03	0.26	0.28	0.46	0.42
R4	0.16	0.48	1.17	1.94	0.29	0.63	0.63	0.50
R5	0.17	0.58	1.25	1.86	0.43	0.50	0.67	0.54
R6	0.19	0.52	1.09	1.64	0.58	0.67	0.68	0.54
R7	0.18	0.47	0.93	1.34	0.62	0.61	0.52	0.44
Bare	0.11	0.22	0.38	0.42	0.78	0.72	0.57	0.53

Table 4: Non-structural acceleration-sensitive components' fragility parameters for the Damage States (DSs): Slight (S), Moderate (M), Extensive (E) and Complete (C).

4 COST ASSESSMENT

This section identifies the repair costs for structural and non-structural components associated with each DS. Since this study focuses on assessing the cost-effectiveness of the retrofit measure, special attention is given to accurately calculating the costs of BRBs. Following this, key metrics are computed as outlined in Section 2, enabling a comparative analysis of the costs associated with bare *vs.* retrofitted structures, as well as the economic advantages of the improved structural performance.

4.1 Buckling Restrain Braces (BRBs) Retrofitting Cost

The cost of each BRB design was evaluated based on the costs of the device, the elastic steel brace, and the installation work required. Costs related to additional retrofit interventions, *e.g.*, foundation reinforcement due to the increased axial forces in the columns within BRB' spans, were excluded from this analysis as it represents a preliminary study. The retrofit cost can be determined as follows:

$$C_R = C_{BRB} + C_{SB} + C_G \tag{6}$$

where C_{BRB} represents the cost of the BRB device, C_{SB} represents the cost of the elastic steel brace, and C_G is the cost of the gusset plates.

The cost of the BRB device can be calculated as follows [41]:

$$C_{BRB} = [0.0124 \cdot A_{BRB}^2 + 1.8702 \cdot A_{BRB} + 10] \cdot \frac{L_{BRB}}{100} \cdot f_{BRB} \tag{7}$$

where A_{BRB} represents the area of the BRB steel core, L_{BRB} is the length of the BRB device, and f_{BRB} is the unit weight cost of BRB in \$/kg, taken equal to 13\$/kg according to FEMA P58 [42].

The cost of the steel brace can be calculated by considering the unit cost of the steel and calculating the weight resulting from the design, as follows:

$$C_{SB} = L_{SteelBrace} \cdot A_{SteelBrace} \cdot \rho_{steel} \cdot f_{steel} \tag{8}$$

where $A_{SteelBrace}$ represents the area of the steel elastic brace, $L_{SteelBrace}$ is the length of the steel elastic brace, ρ_{steel} is the steel specific weight, and f_{steel} is the unit weight cost of steel in \$/kg. The unit cost of steel has been assumed to be \$1.40/kg, based on a market survey.

Finally, the cost of the gusset plates can be determined following FEMA P-58 guidelines. They vary based on the weight of the BRBs (w_{BRB}), as detailed in Table 5.

	w_{BRB}<40kg/m	40<w_{BRB}<90kg/m	w_{BRB}<90kg/m
C_G	750	1500	2500

Table 5: Gusset plate costs, C_G [\$/each].

Figure 3 summarises the resulting BRBs' costs, including the total cost for each retrofit design and the individual costs of the BRBs at each storey. Notably, R1 incurs the highest cost, while R7 is the least expensive, as it uses the smallest BRB sizes.

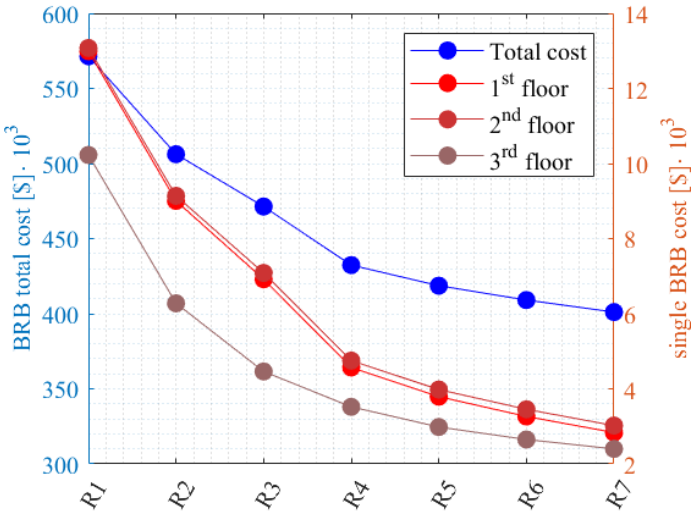

Figure 3: BRBs cost analyses. Total costs refer to the blue left axis while the costs of a single BRB refer to the red right axis.

4.2 Structural and Non-Structural Components Repair Cost

The case study structure is assumed to be an office, *i.e.*, Occupancy Class COM4, according to HAZUS 4.2 [40], with a replacement cost equal to 2200\$/m^2. The HAZUS 4.2 [40] also provides the repair cost, expressed as a percentage of the replacement cost of structural and non-structural components, both acceleration- and drift-sensitive, for different DSs. For structural components, the DSs, defined following ASCE 41-17 [36], were correlated with the DSs outlined in HAZUS [40], which provide repair cost estimates. Specifically, the IO state was linked to HAZUS' Moderate damage state, LS to Extensive, and CP to Complete. The repair cost for each DS as a fraction of the total replacement cost is provided in Table 6.

	Slight	Moderate	Extensive	Complete
Structural	0.4	1.9	9.6	19.2
Non-Structural Drift Sensitive	0.7	3.3	16.4	32.9
Non-Structural Accel. Sensitive	0.9	4.8	14.4	47.9

Table 6: Repair Costs in % of building replacement cost.

4.3 Evaluation and discussion of key metrics

Figure 4 shows the vulnerability functions, illustrating the relationship between the *IM* and the expected replacement cost as a percentage of the total replacement cost. The curve representing the bare structure reaches 100% replacement cost at a significantly lower *IM* value compared to the curves associated with the retrofitted designs (R1–R7).

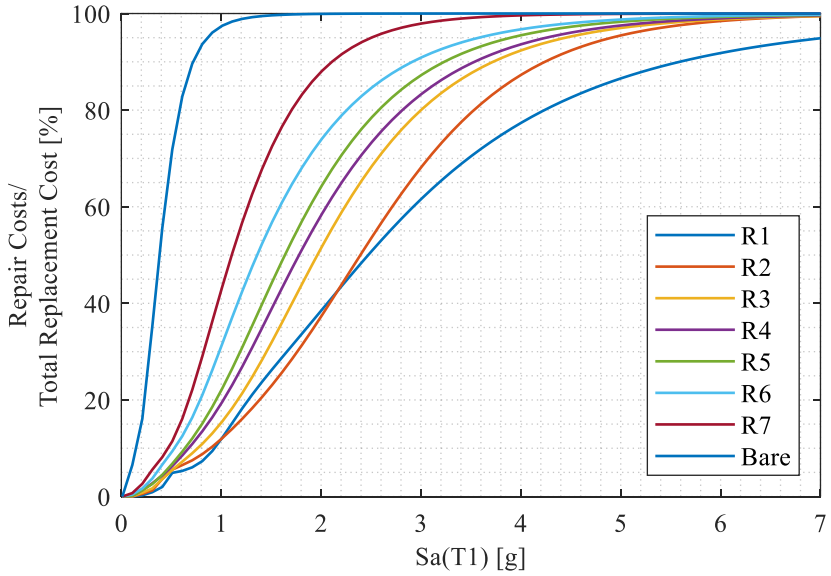

Figure 4: Vulnerability Functions.

The EAL is obtained by convolving the vulnerability functions with the hazard curve for the seven case retrofitted studies and the bare structure. Thereafter, LCC is computed based on an expected lifetime of the building of 50 years, as defined in Eq.

$$\mathrm{LCC} = \frac{(1+r)^{T_N}-1}{r} \cdot \mathrm{EAL} + C_R \tag{4}$$

(2).

Figure 5 and Table 7 present the values of EAL, LCC, and ROI for both the bare and retrofitted structures. The bare structure exhibits the highest EAL and LCC, significantly exceeding those of the retrofitted models. For instance, the LCC of the bare structure accounts for nearly 70% of the total replacement cost, whereas the LCC of the retrofitted solutions is slightly more than 40%. This highlights its extreme susceptibility to seismic damage and the high financial burden of potential repairs or replacement. Conversely, the retrofitted structures show considerably lower EAL and LCC values, demonstrating the effectiveness of retrofitting in reducing expected seismic losses.

Although all retrofitted structures demonstrate higher performance than the bare structure, the variability in EAL and LCC values is notable. Some models (*e.g.,* R5 and R6) appear to achieve better cost efficiency, evidenced by a slight reduction in values compared to others. This is also evident considering the ROI reported in Table 7. It is worth highlighting that R1 and R5 have comparable LCC. However, it is expected that accounting for additional costs associated with the retrofitting, *e.g.,* foundation reinforcement, would lead to higher LCC for the R1 design, highlighting the benefits of other designs.

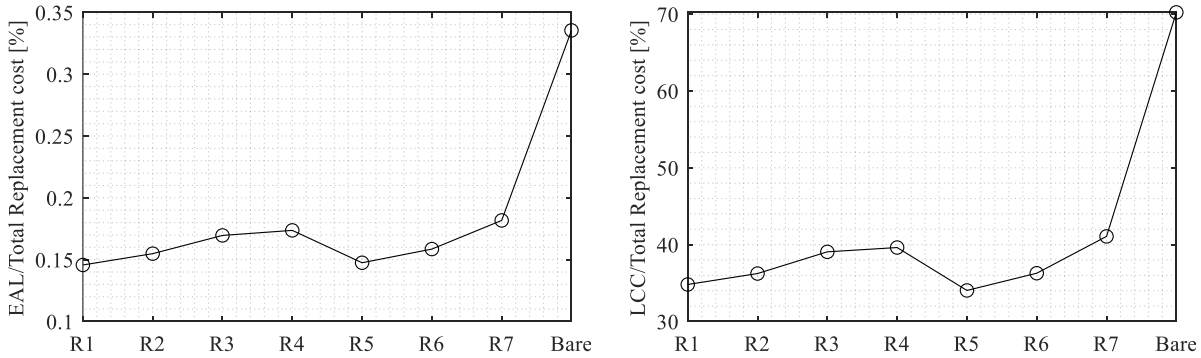

Figure 5: a) Expected Annual Loss (EAL) and b) Life Cycle Cost (LCC) of the retrofitted and bare structures.

	R1	R2	R3	R4	R5	R6	R7	Bare
EAL [$]	17782	19095	21274	22090	18909	20661	24603	54436
LCC [$]	4611769	4800253	5174515	5248654	4508830	4805979	5440748	9302933
ROI [y]	24.30	23.29	23.48	22.63	20.21	20.70	22.30	/

Table 7: Key metrics values: Expected Annual Loss (EAL), Life Cycle Cost (LCC) and Return on Investment (ROI) of the retrofitted and bare structures.

Additionally, the retrofit designs are compared through the BCR, which defines the ratio of the benefits gained and the costs incurred, as outlined in Section 2. Figure 6 shows the BCR for the retrofitted structures. While R1 is the most effective at minimising the fragility, its high retrofitting costs result in the lowest BCR among all designs. This implies that, despite significant safety enhancements, R1 is not the most economically efficient option. In contrast, design R7 exhibits a relatively high BCR. Although it does not drastically reduce the structural fragility, its low retrofitting cost makes it a financially attractive alternative. R5 stands out with the highest BCR (~11.5), striking the best balance between cost and benefit by delivering considerable fragility reduction without incurring excessive retrofitting expenses. Moreover, when analysing the ROI, R5 outperforms R1 by up to 20%, which is a substantial margin in terms of investment.

Figure 7 summarises all the key metrics investigated in the form of a radar chartFigure **7**: Summary of key metrics adopted to compare bare and retrofitted structures.. This visualization allows highlighting the benefits of design R5 in achieving the most cost-effective balance

among all the considered metrics. Specifically, it maximises the BCR, minimises both the LCC and ROI, and maintains sufficiently low initial costs.

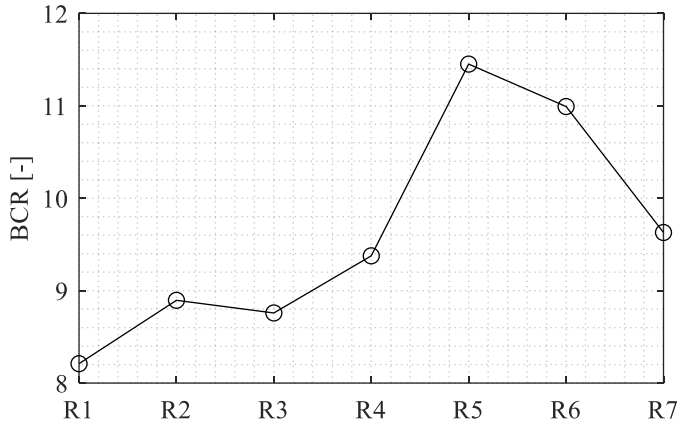

Figure 6: Benefit-to-cost ratio (BCR).

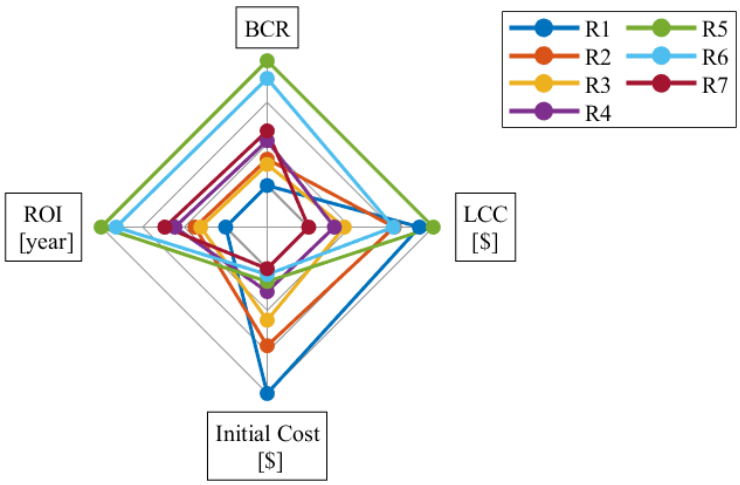

Figure 7: Summary of key metrics adopted to compare bare and retrofitted structures.

5 CONCLUSIONS

This study investigates the seismic performance of non-seismically designed steel Moment-Resisting Frames (MRFs) and evaluates the efficiency of Buckling Restrained Braces (BRBs) as retrofitting designs. It examines various BRB designs and their economic impact through a Life-Cycle Cost (LCC) analysis, which includes retrofitting and potential repair costs following major seismic events. By performing a multi-parameter analysis, the research identifies the most cost-effective BRB design using key metrics, including Expected Annual Loss (EAL), Life Cycle Cost (LCC), Benefit-to-Cost Ratio (BCR), and Return on Investment (ROI). This methodology allows for a comparison between different retrofit designs, highlighting the strengths and weaknesses of each and avoiding biased decisions based on single-parameter evaluations, *e.g.*, risk reduction or LCC.

The findings highlight that the investigated retrofit strategy, *i.e.*, the use of BRBs, substantially reduces both structural and non-structural damage, resulting in a notable decrease in EAL and overall LCC. Among the examined designs, retrofitting designs that balance structural protection and economic feasibility, such as R5 and R6, demonstrate the highest BCR, making them the most financially viable options. Although the R1 design offers the highest level of

seismic risk reduction, its elevated initial investment cost results in a lower economic return. Conversely, designs such as R7, while cost-efficient in terms of installation, exhibit a comparatively lower reduction in seismic vulnerability, which may lead to increased long-term financial burdens.

The study reinforces the importance of integrating seismic risk assessment with economic analysis when selecting retrofitting solutions. Decision-makers should consider not only the initial retrofitting cost and standardised safety objectives but also the long-term benefits, including reduced repair and replacement expenses. Future developments could enhance the LCC analysis by improving cost accuracy. These refinements should account for additional components of the structural strengthening costs and consider component-specific repair costs.

REFERENCES

[1] Crowley H, Despotaki V, Silva V, Dabbeek J, Romão X, Pereira N, et al. Model of seismic design lateral force levels for the existing reinforced concrete European building stock. *Bulletin of Earthquake Engineering*, **19**, 2839–65, 2021.

[2] Buckle IG, Mayes RL. Seismic Isolation: History, Application, and Performance—A World View. *Earthquake Spectra* **6,** 161–201, 1990.

[3] Mokha AS, Amin N, Constantinou MC, Zayas V. Seismic Isolation Retrofit of Large Historic Building. *Journal of Structural Engineering*, **122,** 298–308, 1996.

[4] Charmpis DC, Phocas MC, Komodromos P. Optimized retrofit of multi-storey buildings using seismic isolation at various elevations: assessment for several earthquake excitations. *Bulletin of Earthquake Engineering*, **13,** 2745–68, 2015.

[5] Xie Q. State of the art of buckling-restrained braces in Asia. *Journal of Constructional Steel Research*, **61**, 727–48, 2005.

[6] Di Sarno L, Elnashai AS. Bracing systems for seismic retrofitting of steel frames. *Journal of Constructional Steel Research*, **65**, 452–65, 2009.

[7] Andreotti R, Giuliani G, Tondini N. Experimental analysis of a full-scale steel frame with replaceable dissipative connections. *Journal of Constructional Steel Research*, **208,** 108036, 2023.

[8] Xia C, Hanson RD. Influence of ADAS Element Parameters on Building Seismic Response. *Journal of Structural Engineering*, **118,** 1903–18, 1992.

[9] Benedetti A, Landi L, Merenda DG. Displacement-Based Design of an Energy Dissipating System for Seismic Upgrading of Existing Masonry Structures. *Journal of Earthquake Engineering*, **18**, 477–501, 2014.

[10] Tsai K-C, Chen H-W, Hong C-P, Su Y-F. Design of Steel Triangular Plate Energy Absorbers for Seismic-Resistant Construction. *Earthquake Spectra*, **9,** 505–28, 1993.

[11] TahamouliRoudsari M, Eslamimanesh MB, Entezari AR, Noori O, Torkaman M. Experimental Assessment of Retrofitting RC Moment Resisting Frames with ADAS and TADAS Yielding Dampers. *Structures*, **14,** 75–87, 2018.

[12] Freddi F, Galasso C, Cremen G, Dall'Asta A, Di Sarno L, Giaralis A, et al. Innovations in earthquake risk reduction for resilience: Recent advances and challenges. International *Journal of Disaster Risk Reduction*, **60,** 102267, 2021.

[13] Black CJ, Makris N, Aiken ID. Component Testing, Seismic Evaluation and Characterization of Buckling-Restrained Braces. *Journal of Structural Engineering*, **130,** 880–94, 2004.

[14] Zona A, Dall'Asta A. Elastoplastic model for steel buckling-restrained braces. *Journal of Constructional Steel Research*, **68,** 118–25, 2012.

[15] Sutcu F, Bal A, Fujishita K, Matsui R, Celik OC, Takeuchi T. Experimental and analytical studies of sub-standard RC frames retrofitted with buckling-restrained braces and steel frames. *Bulletin of Earthquake Engineering,* **18,** 2389–410, 2020.

[16] Freddi F, Wu J, Cicia M, Di Sarno L, D'Aniello M, Gutiérrez-Urzúa F, et al. Seismic Retrofitting of Existing Steel Frames with External BRBs: Pseudo-Dynamic Hybrid Testing and Numerical Parametric Analysis. *Earthquake Engineering & Structural Dynamics*, **54,** 1064–83, 2025.

[17] Güneyisi EM. Seismic reliability of steel moment resisting framed buildings retrofitted with buckling restrained braces. *Earthquake Engineering & Structural Dynamics*, **41,** 853–74, 2012.

[18] Sutcu F, Takeuchi T, Matsui R. Seismic retrofit design method for RC buildings using buckling-restrained braces and steel frames. *Journal of Constructional Steel Research*, **101,** 304–13, 2014.

[19] Velasco L, Hospitaler A, Guerrero H. Optimal design of the seismic retrofitting of reinforced concrete framed structures using BRBs. *Bulletin of Earthquake Engineering*, **20,** 5135–60, 2022.

[20] Gutiérrez-Urzúa F, Freddi F. Influence of the design objectives on the seismic performance of steel moment resisting frames retrofitted with buckling restrained braces. *Earthquake Engineering & Structural Dynamics,* **51,** 3131–53, 2022.

[21] Chelapramkandy R, Ghosh J, Freddi F. Influence of masonry infills on seismic performance of BRB-retrofitted low-ductile RC frames. *Earthquake Engineering & Structural Dynamics,* **54,** 295–318, 2025.

[22] Gutiérrez-Urzúa F, Freddi F, Tubaldi E. Seismic risk and failure modes assessment of steel BRB frames under earthquake sequences. *Structural Safety*, 102598, 2025.

[23] Mitropoulou CCh, Lagaros ND, Papadrakakis M. Life-cycle cost assessment of optimally designed reinforced concrete buildings under seismic actions. *Reliability Engineering & System Safety* **96**, 1311–31, 2011.

[24] Liu M, Burns SA, Wen YK. Optimal seismic design of steel frame buildings based on life cycle cost considerations. *Earthquake Engineering & Structural Dynamics,* **32**, 1313–32, 2003.

[25] Vitiello U, Asprone D, Di Ludovico M, Prota A. Life-cycle cost optimization of the seismic retrofit of existing RC structures. *Bulletin of Earthquake Engineering,* **15**, 2245–71, 2017.

[26] Padgett JE, Dennemann K, Ghosh J. Risk-based seismic life-cycle cost–benefit (LCC-B) analysis for bridge retrofit assessment. *Structural Safety*, **32**, 165–73, 2010.

[27] Liel AB, Deierlein GG. Cost-Benefit Evaluation of Seismic Risk Mitigation Alternatives for Older Concrete Frame Buildings. *Earthquake Spectra*, **29**, 1391–411, 2013.

[28] Sousa L, Monteiro R. Seismic retrofit options for non-structural building partition walls: Impact on loss estimation and cost-benefit analysis. *Engineering Structures*, **161,** 8–27, 2018.

[29] McKenna F, Fenves G, Scott M. *OpenSees: Open System for Earthquake Engineering Simulation.* University of California Berkeley 2006.

[30] Fajfar P. A Nonlinear Analysis Method for Performance-Based Seismic Design. *Earthquake Spectra*, **16,** 573–92, 2000.

[31] Ragni L, Zona A, Dall'Asta A. Analytical expressions for preliminary design of dissipative bracing systems in steel frames. *Journal of Constructional Steel Research*, **67**, 102–13, 2011.

[32] Freddi F, Tubaldi E, Ragni L, Dall'Asta A. Probabilistic performance assessment of low-ductility reinforced concrete frames retrofitted with dissipative braces. *Earthquake Engineering & Structural Dynamics*, **42**, 993–1011, 2013.

[33] Vamvatsikos D, Cornell CA. Incremental dynamic analysis. *Earthquake Engineering & Structural Dynamics*, **31**, 491–514, 2002. https://doi.org/10.1002/eqe.141.

[34] Baker JW. Efficient Analytical Fragility Function Fitting Using Dynamic Structural Analysis. *Earthquake Spectra*, **31**, 579–99, 2015.

[35] Gupta A, Krawinkler H. Behavior of ductile SMRFs at various seismic hazard levels. *Journal of Structural Engineering*, **126**, 98–107, 2000.

[36] Structural Engineering Institute. *ASCE/SEI, 41-17: seismic evaluation and retrofit of existing buildings.* American Society of Civil Engineers, 2017.

[37] Lignos DG, Krawinkler H. Deterioration modeling of steel components in support of collapse prediction of steel moment frames under earthquake loading. *Journal of Structural Engineering*, **137**, 1291–302, 2011.

[38] Zareian F, Medina RA. A practical method for proper modeling of structural damping in inelastic plane structural systems. *Computers & Structures*, **88**, 45–53, 2010.

[39] Castro J, Elghazouli A, Izzuddin B. Modelling of the panel zone in steel and composite moment frames. *Engineering Structures*, **27**, 129–44, 2005.

[40] Federal Emergency Management Agency (FEMA). *Hazus Earthquake Model Technical Manual. Hazus 4.2*. 2020.

[41] Ahmadie Amiri H, Estekanchi HE. Life cycle cost-based optimization framework for seismic design and target safety quantification of dual steel buildings with buckling-restrained braces. *Earthquake Engineering & Structural Dynamics*, **52**, 4048–81, 2023.

[42] Federal Emergency Management Agency (FEMA). *FEMA P-58. Seismic Performance Assessment of Buildings*. 2018.